



Cite this: *RSC Adv.*, 2020, 10, 3005

# The efficient biogenesis of Ag and NiO nanoparticles from VPLE and a study of the anti-diabetic properties of the extract

Hongying Gao,<sup>a</sup> Reza Tayebiee,<sup>b</sup>  <sup>\*,b</sup> Mojtaba Fattahi Abdizadeh,<sup>\*cd</sup> Esrafil Mansouri,<sup>e</sup> Maryam Latifnia<sup>f</sup> and Zahra Pourmojhed<sup>g</sup>

*Vitex pseudo-negundo* leaf extract (VPLE) is used to mediate the green biosynthesis of Ag and NiO nanoparticles in aqueous solutions under mild conditions. The synthesized nanoparticles, with a narrow size range and good distribution, are characterized by means of powder X-ray diffraction (PXRD), Fourier-transform infrared (FT-IR), scanning electron microscopy (SEM), energy-dispersive X-ray spectroscopy (EDX), and transmission electron microscopy (TEM) techniques. SEM and TEM micrographs proved formation of mostly spherical or ellipsoidal nanoparticles with little agglomeration, and the average particle size was less than 20–35 nm for both types of nanoparticle. Then, the protective role of VPLE toward the liver is assessed in streptozotocin-induced diabetic rats. For this purpose, diabetes is induced in rats through the intraperitoneal injection of streptozotocin, and VPLE is administered *via* oral gavage for 6 weeks. This study suggests that VPLE can ameliorate biochemical and structural changes in the livers of diabetic rats, showing that VPLE can improve the condition of rats with diabetic hepatopathy *via* a decrease in oxidative stress and an enhancement in the activity of antioxidant enzymes in the liver.

Received 22nd October 2019  
Accepted 6th December 2019

DOI: 10.1039/c9ra08668d

rsc.li/rsc-advances

## 1. Introduction

Nanomedicine and nanobiotechnology are emerging fields of nanoscience that utilize therapeutic nanoparticles for various biomedical applications.<sup>1</sup> The green facilitated synthesis of metallic and metal oxide nanoparticles is an important and growing objective in the nanotechnology field due to the unusual optical, chemical, photochemical and electronic properties of the fabricated nanoparticles.<sup>2</sup> Among the various novel eco-friendly scenarios for the production of nanoparticles, plant extracts possess a wide range of biologically active compounds, which have been exploited as top resources for the green synthesis of nanoparticles.<sup>3,4</sup> These biosynthetic methods have received more attention than common chemical and physical methodologies due to their ease of synthesis and

their eco-friendly and cost-effective nature.<sup>5–9</sup> Therefore, biological resources can be used in rapid, effective, simple, and economic ways to produce desired nanoparticles.<sup>10</sup> Furthermore, plant extracts behave as both capping and reducing agents during biosynthesis; therefore, these biotemplates can control the sizes, shapes, and morphologies of the prepared nanoparticles through rendering a coordination sphere for capturing metal ions.<sup>11</sup> Among the various available nanoparticles, silver and NiO nanoparticles have attracted wide interest due to their numerous applications in industry and academia. Silver nanoparticles have widespread applications in non-linear optics, biolabelling, and optical receptors, as well as in dentistry, catalysis, and the food industry.<sup>12</sup> Furthermore, NiO nanoparticles also have a number of important applications in energy storage devices,<sup>13</sup> drug delivery, and magnetic resonance imaging.<sup>14</sup> Therefore, developing efficient and simple methods for the fabrication of Ag and NiO nanoparticles with controlled size is a favorable target for many scholars.

*Vitex pseudo-negundo* (VPN) is a familiar herb that commonly grows in wasteland as a hedge plant. Numerous studies have shown that the roots, flowers, fruits, and leaves of this plant have great medicinal benefits. The leaves of VPN contain flavonoids, alkaloids, monoterpenes, eustroside, saturated steroidal and triterpinoidal saponins, amino acids, and aromatic amines.<sup>15</sup> This herb is traditionally utilized to cure and treat many deficiencies, such as amenorrhea, corpus luteum insufficiency, dysmenorrhea, hyperprolactinemia, and breast-feeding disorders.<sup>16,17</sup> Moreover, extracts from different parts of

<sup>a</sup>Department of Chinese Medicine, Binzhou City Central Hospital, Binzhou, Shandong Province, 251700, China

<sup>b</sup>Department of Chemistry, School of Sciences, Hakim Sabzevari University, Sabzevar, 96179-76487, Iran. E-mail: rtayebiee@hsu.ac.ir

<sup>c</sup>Department of Lab Sciences, Faculty of Paramedicine, Sabzevar University of Medical Sciences, Sabzevar, Iran. E-mail: mojtabafattahi@gmail.com

<sup>d</sup>Cellular and Molecular Research Center, Sabzevar University of Medical Sciences, Sabzevar, Iran

<sup>e</sup>Department of Anatomical Sciences, Cellular and Molecular Research Center, Faculty of Medicine, Ahvaz Jundishapur University of Medical Sciences, Ahvaz, Iran

<sup>f</sup>Department of Gastrointestinal and Liver Disease, Faculty of Medicine, Sabzevar University of Medical Sciences, Sabzevar, Iran

<sup>g</sup>Diabetes Clinic, Sabzevar University of Medical Sciences, Sabzevar, Iran


this plant have antibacterial,<sup>18</sup> anti-inflammatory,<sup>19</sup> anti-diabetic,<sup>20</sup> antioxidant,<sup>21</sup> anti-fungal,<sup>22</sup> and anti-HIV<sup>23</sup> activities. Recently, this herb was reported to show cytotoxic activity against a human breast cancer cell line.<sup>24</sup> In a continuation of our previous studies,<sup>25</sup> herein, the use of the leaf extract of this plant is demonstrated for the environmentally friendly, fast, cost-effective, and one-step synthesis of Ag and NiO nanoparticles under ambient conditions and without any external additives.

The antidiabetic activities and effects of different nanoparticles on various tissue injuries and tumors are of interest, and they have been investigated by several research groups.<sup>26–32</sup> Diabetes mellitus (DM), which is characterized by the existence of chronic hyperglycemia, is known as one of the five main causes of death.<sup>33–35</sup> Liver disease is considered as one of the major complications related to oxidative stress disorders like DM<sup>36</sup> and ethological studies have provided many evidence that chronic hyperglycemia causes complicated diabetic hepatopathy.<sup>37,38</sup> Oxidative stress provides an effective mechanism by which the glycation process, a precise enzyme-controlled process related to glucose metabolism, the hyper-production of free-radical precursors, and a decrease in the efficiency of antioxidants all contribute to a surge in disease severity.<sup>37,39</sup> It has been shown that *Vitex* constituents have protective effects against experimentally induced diabetic complications through increasing the antioxidant enzyme activity. VPN is a studied model that has been employed to produce multiple effective remedies.<sup>40–44</sup> We evaluated the hypoglycemic effects of VPLe in an induced diabetes animal model using Wistar male rats. Furthermore, this study examined some potentially important clinical parameters, including antioxidant activities and lipid peroxidation, related to streptozotocin-induced diabetic hepatopathy in the livers of rats and compared the results with treated and untreated groups. The effects of VPLe treatment on liver function in the affected rats were also evaluated. The findings of the present study may provide new alternative herbal medicine approaches for controlling diabetic complications in humans.

## 2. Results and discussion

### 2.1. Morphological and characterization studies

The reduction of  $\text{Ag}^+$  and  $\text{Ni}^{2+}$  ions into nanoparticles was easily demonstrated *via* the distinct color change from pale yellow-green to dark brown and yellow, respectively. Color changes in aqueous solutions of nanoparticles are due to surface plasmon resonance phenomena. Obviously, the formation of mostly stable complexes between nanoparticles and effective plant extract functional groups can stabilize the prepared particles.<sup>45,46</sup> To examine the elemental compositions of the NiO and Ag nanoparticles and ensure the absence of organic elements originating from the plant extract, EDX analysis was conducted (Fig. 1). The obtained profiles of the synthesized nanoparticles confirmed the major presence of only nickel, oxygen, and Ag in the nanoparticles, without any other impurities.

Fig. 2 displays the PXRD patterns of NiO and Ag nanoparticles fabricated using VPLe under the outlined experimental conditions. Five sharp and intense Bragg reflections were observed with maxima centered at  $2\theta$  values of  $37.4^\circ$ ,  $43.4^\circ$ ,  $63.1^\circ$ ,  $75.4^\circ$ , and  $79.5^\circ$  due to the (111), (200), (220), (311) and (222) crystal planes, respectively, of cubic NiO (JCPDS card no. 73-1523) (Fig. 2a). Using the Debye–Scherrer equation, the average size of the NiO nanoparticles was found to be 17–25 nm. Fig. 2b depicts the wide-angle PXRD pattern of the Ag nanoparticles, showing diffraction peaks at  $38.2^\circ$ ,  $44.5^\circ$ ,  $64.6^\circ$ ,  $77.5^\circ$ , and  $81.7^\circ$  related, respectively, to the 111, 200, 220, 311, and 222 crystallographic planes of face centered cubic Ag (JCPDS card no. 01-087-0719).<sup>47,48</sup> Clearly, the Ag nanoparticles were crystalline and no other impurity phases were found. An average particle size of less than 20 nm was calculated using the Debye–Scherrer equation for the Ag nanoparticles.

Fig. 3 shows the FT-IR spectra of NiO and Ag nanoparticles in the spectral range of  $500\text{--}4000\text{ cm}^{-1}$  after simple calcination to remove the organic components from the leaf extract. The characteristic vibration bands in Fig. 3a at around  $500\text{--}650\text{ cm}^{-1}$  are distinctive modes from the NiO phase due to metal–oxygen stretching.<sup>49</sup> Additional bands at  $\sim 3500\text{ cm}^{-1}$  and  $1300\text{--}1600\text{ cm}^{-1}$  are due to adsorbed water molecules and surface hydroxyl groups, respectively. It should be mentioned

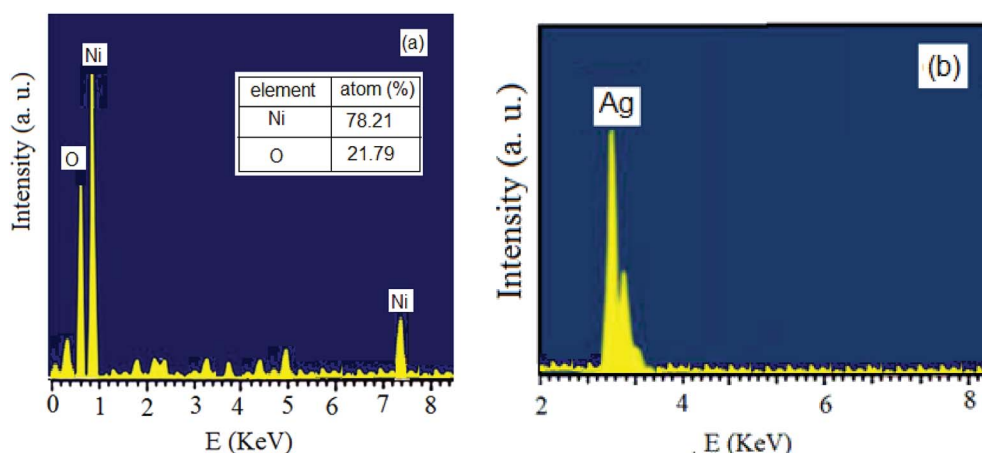


Fig. 1 The EDX patterns from (a) NiO and (b) Ag nanoparticles.



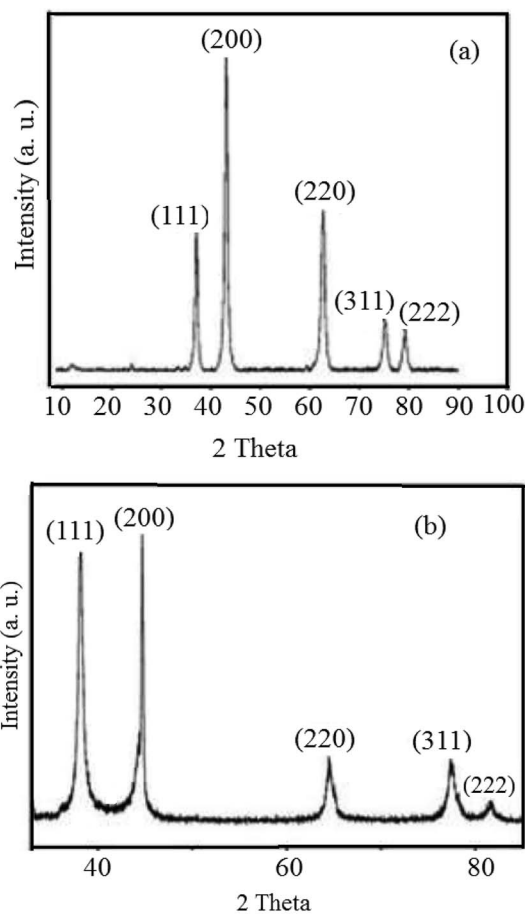


Fig. 2 The PXRD patterns of (a) NiO and (b) Ag nanoparticles.

that the non-appearance of any functional groups due to biomolecules from VPLe confirmed the complete combustion of the organic shell materials around the nanoparticles. Fig. 3b shows the FT-IR spectrum of the Ag nanoparticles prepared using VPLe. The interaction of the Ag nanoparticles with the shell biomolecules leads to strong and clear peaks at around  $1350\text{--}1650\text{ cm}^{-1}$ . The strong peak at  $\sim 650\text{ cm}^{-1}$  is a characteristic band from Ag nanoparticles. Moreover, a strong and broad band was observed at around  $3400\text{ cm}^{-1}$  in the spectra of both the NiO and Ag nanoparticles, which should be assigned to the hydroxyl groups of adsorbed water molecules.

The surface morphology of the synthesized NiO nanoparticles was studied *via* SEM (Fig. 4b). The particles were almost spherical in shape and some agglomeration was detected. The SEM image in Fig. 4a shows the morphology of the Ag nanoparticles, confirming the presence of almost ellipsoid Ag nanoparticles. The morphologies and sizes of the NiO and Ag nanoparticles were also determined *via* TEM (Fig. 5). This study confirmed the narrow particle distributions. Fig. 5a shows that the Ag nanoparticles have an almost spherical shape and are well-dispersed. The TEM image reveals a mean diameter of less than 20 nm for the Ag nanoparticles.

## 2.2. Studying the protective role of VPLe in the livers of streptozotocin-induced diabetic rats

The present study examined the liver-protecting effects of VPLe in an STZ-induced diabetic hepatopathy model. Similar to previous research using other herbal extracts,<sup>50</sup> our results indicated that VPLe successfully improved and regulated the FBS, ALT, AST, ALP and Alb levels in diabetic rats at significant levels compared to those left untreated by VPLe (Table 1). We demonstrated that  $500\text{ mg kg}^{-1}$  VPLe was more effective than  $250\text{ mg kg}^{-1}$ . The obtained results suggest that VPLe has hypoglycemic activity. These observations validate and support the traditional use of VPLe against such diseases.

The initial and most important indicators for assessing liver injury are the levels of ALT, AST, ALP and Alb. A probable mechanism explaining the above-mentioned effects would be disturbances in the cellular architecture of diabetics, evoked by severe pro-oxidative stress.<sup>38,39</sup> The production of oxidants can induce apoptosis in hepatocytes and can induce oxidative stress, which is an indicator of these disturbances.<sup>38</sup> Notably, it is found that hyperglycemia decreases the synthesis and activity of some antioxidizing enzymes, such as SOD and GPx, likely *via* a glycation process.

In the present study, like other studies<sup>51,52</sup> using liver-protecting herbal extracts, we demonstrated that VPLe considerably reduced lipid peroxidation and increased the activities of SOD and GPx in diabetic rats compared to healthy controls (Table 2). VPLe played a protective role against experimentally induced diabetic hepatopathy, which may be due to the inhibition of AGE formation. The inhibitory effects of VPLe could be related to the antioxidant activity of VPLe.<sup>38,53,54</sup> The remarkable free radical scavenging activity of VPLe could be a potential

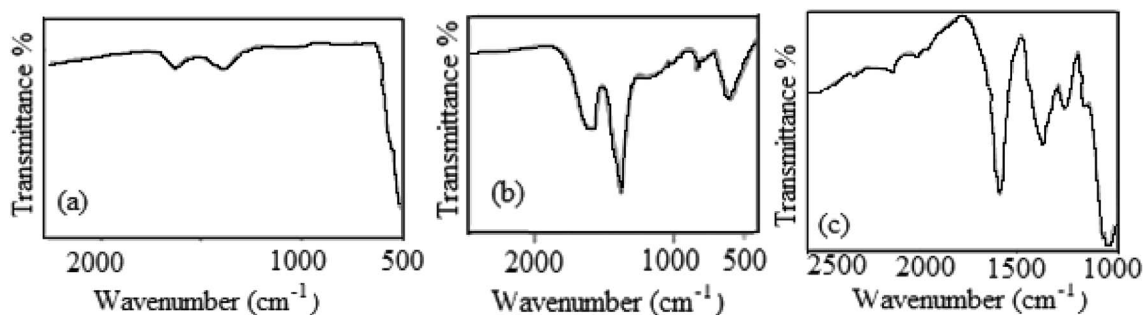


Fig. 3 The FT-IR spectra of the synthesized (a) NiO and (b) Ag nanoparticles, and VPLe (c).



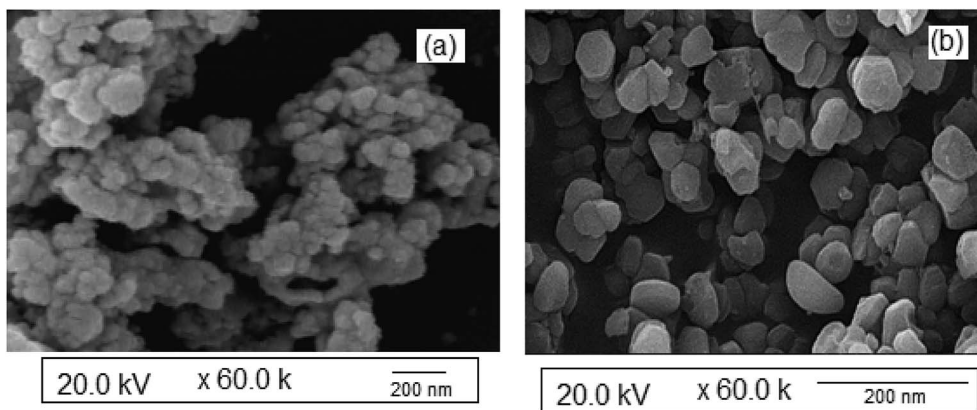


Fig. 4 SEM images of (a) Ag and (b) NiO nanoparticles.

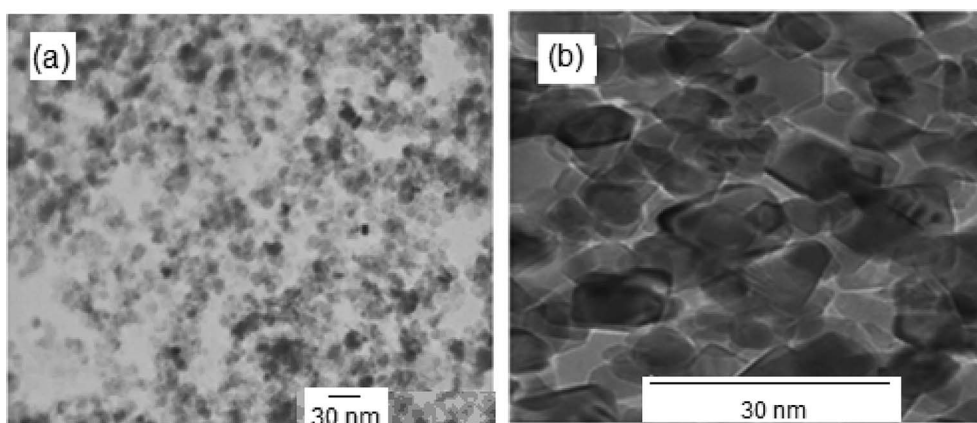


Fig. 5 TEM images of (a) Ag and (b) NiO nanoparticles.

reason for its effects on reversing lipid peroxidation levels and on the antioxidant activities of SOD and GPx enzymes.

Considering hepatopathy as one of the most important diabetes-induced complications,<sup>38,55</sup> we performed histological examinations of H&E stained liver samples and tested pathological tissue variations. Histopathological examinations revealed that VPLe administration (either at a dose of 250 or 500 mg kg<sup>-1</sup>) may reverse the degeneration of liver tissue structures and lead to the reappearance of hyperplastic

hepatocytes in damaged liver, as shown in Fig. 6c and d. On the other hand, mild to rigorous destruction, cellular abnormalities with areas of vascular degeneration, necrosis, and cellular degeneration were detected in liver samples from STZ-induced diabetic rats, compared to the normal control group (Fig. 6b). These findings are consistent with a previous study<sup>56</sup> that reported the positive effects of *Vitex negundo*, which is botanically close to VPN, on liver tissue.

**Table 1** The effects of 6 weeks of VLHE administration (250 and 500 mg kg<sup>-1</sup>) on the fasting blood sugar and serum biomarker levels relating to the liver function of normal and streptozotocin-induced diabetic rats<sup>a</sup>

Parameter	Group			
	Healthy control	Diabetic control	VLHE (250 mg kg <sup>-1</sup> )	VLHE (500 mg kg <sup>-1</sup> )
GLU (mg dl <sup>-1</sup> )	94.4 ± 7.54	366.2 ± 139.26*	148.5 ± 20.21**	139 ± 28.91**
ALT (U/l)	64.2 ± 11.0	145 ± 18.15*	80.4 ± 5.94**	72.6 ± 5.13**
AST (U/l)	115.2 ± 10.91	205 ± 32.18*	136.4 ± 11.97**	119.8 ± 17.72**
ALP (U/l)	112.8 ± 12.9	237 ± 58.83*	140 ± 12.16**	117.6 ± 7.7**
Alb (g dl <sup>-1</sup> )	3.73 ± 0.26	2.19 ± 0.27*	2.876 ± 0.24**	3.062 ± 0.26**

<sup>a</sup> Results are expressed as mean ± SE (n = 5); \* means in diabetic and healthy control groups are significantly different from each other (P < 0.01); \*\* means in diabetic + VLHE (250 and 500 mg kg<sup>-1</sup>) and diabetic groups are significantly different from each other (P < 0.05).





**Table 2** The effects of 6 weeks of VLHE administration (250 and 500 mg kg<sup>-1</sup>) on the antioxidant enzyme activities in the livers of normal and streptozotocin-induced diabetic rats<sup>a</sup>

Parameter	Group			
	Healthy control	Diabetic control	VLHE (250 mg kg <sup>-1</sup> )	VLHE (500 mg kg <sup>-1</sup> )
GPx	19.79 ± 0.60	10.44 ± 1.06*	18.18 ± 1.02**	18.24 ± 1.60**
SOD	17.09 ± 0.78	11.80 ± 0.75*	16.54 ± 0.47**	16.93 ± 0.43**
MDA	17.43 ± 1.09	30.18 ± 2.19*	21.18 ± 1.29**	20.10 ± 1.36**

<sup>a</sup> Results are expressed as mean ± SE (*n* = 5); \* means in diabetic and healthy control groups are significantly different from each other (*P* < 0.01); \*\* means in diabetic + VLHE (250 and 500 mg kg<sup>-1</sup>) and diabetic groups are significantly different from each other (*P* < 0.05).

The results in Fig. 6 demonstrate that VPLE at a dose of 250 mg kg<sup>-1</sup> leads to some improvements in liver tissue, with moderate areas of cellular restoration and pyknotic nuclei compared to normal and diabetic control groups; however, the destruction of liver structures was still visible (Fig. 6c). On the other hand, 500 mg kg<sup>-1</sup> VPLE completely reversed cellular architecture degeneration and led to the reappearance of hyperplastic hepatocytes in the damaged liver (Fig. 6d).

### 3. Experimental

#### 3.1. Materials, methods, and characterization techniques

Grown leaves of VPN were collected from Sabzevar Province, situated in the east of Iran, during the flowering stage at a rain-free time, and they were air-dried at ambient temperature. AgNO<sub>3</sub> (99.98%), nickel nitrate hexahydrate (99.98%), and

methanol (CH<sub>3</sub>OH, 99.9%) were purchased from Merck (Germany). All aqueous solutions were prepared using double-distilled water. Fourier transform infrared (FT-IR) spectra were obtained using an 8700 Shimadzu Fourier transform spectrophotometer in the form of diluted samples (10 wt%) pressed into KBr pellets. PXRD patterns of the prepared nanoparticles were obtained using a computer controlled STOE diffractometer with monochromatic Cu Kα radiation ( $\lambda$  = 1.5406 Å), operating at a voltage and current of 40 kV and 35 mA, respectively, in the angular range of 0–90°. The morphologies and structures of the expected nanoparticles were studied by means of a field emission scanning electron microscope (JEOL, Model JFC-1600) and transmission electron microscope (PHILIPS TECNAI 10) equipped with an energy dispersive X-ray (EDX) analysis instrument.

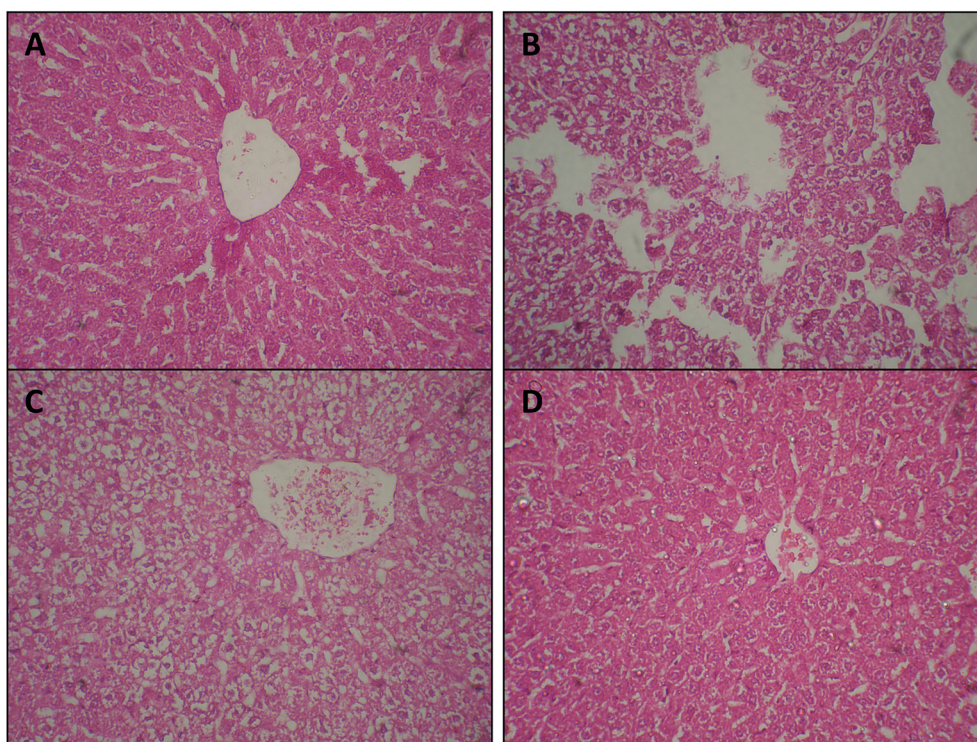


**Fig. 6** Histopathology examinations of liver tissue from different groups: (A) healthy control rat; (B) diabetic control rat; (C) VPLE-treated rat (250 mg kg<sup>-1</sup> body weight); and (D) VPLE-treated rat (500 mg kg<sup>-1</sup> body weight); H&E, 300×.



### 3.2. Preparation of nickel oxide nanoparticles

Air-dried VPN leaves (100 g) were blended with deionized water (1000 ml) in a Clevenger-type apparatus. Then, the obtained green aqueous solution was heated to about 100 °C for 1.5 h. The natural extract solution was filtered properly. Nickel nitrate hexahydrate was used as the nickel precursor without any further purification. In a typical procedure, 20 ml of VPN plant aqueous extract was mixed dropwise with 75 ml of 0.1 mM aqueous  $\text{Ni}(\text{NO}_3)_2$  solution under constant stirring at 80 °C for 2 h. Then, the solution was evaporated gently, and the obtained dark green-brown precipitate was transferred to a ceramic container and heated to 400 °C in a furnace for 10 h to obtain an annealed light-yellow powder.

### 3.3. Preparation of silver nanoparticles

Typically, 5 ml of aqueous extract solution was added to 50 ml of 1 mM silver nitrate solution under vigorous stirring at room temperature for 2 h. Finally, the obtained Ag nanoparticles were separated *via* two centrifugation runs at 10 000 rpm for 30 min at 4 °C.

### 3.4. Animal model

Forty healthy Wistar male rats were selected and kept at the animal house of the Sabzevar University of Medical Science under the standard acclimatization conditions ( $22 \pm 3$  °C, 12 h light/dark cycle). Then, they were fed, acclimatized, and maintained based on rodent diet guidelines issued by the International Council of Laboratory Animal Science (ICLAS). Their weight was between 180 and 200 g at the time of study.

**3.4.1. Ethics statement.** All animal procedures were performed in strict accordance with the Guidelines for the Care and Use of Laboratory Animals of Sabzevar University of Medical Sciences and experiments were approved by the Animal Ethics Committee of Sabzevar University of Medical Sciences, Sabzevar, Iran (approval ID: IR. Medsab, Rec.1393.55, 393040166). In all experimental procedures, efforts were made to minimize pain and suffering.

### 3.5. Studying the protective role of VPLe in the livers of streptozotocin-induced diabetic rats

Forty Wistar male rats were divided into four groups, with ten animals in each group. These included a healthy control group, an untreated streptozotocin-induced diabetic group, and treated diabetic groups, which were separately treated with 250 and 500  $\text{mg kg}^{-1}$  VPLe, respectively, *via* oral gavage for a 6 week period. Diabetes was induced in rats *via* the intraperitoneal injection of STZ (Sigma, Millstone, USA) ( $45 \text{ mg kg}^{-1}$ ). All rats that showed fasting blood sugar levels of above 200  $\text{mg dl}^{-1}$  were considered as diabetic.

**3.5.1. Biochemical examination.** On the last day of experiment, five rats were randomly selected from each group and these were sacrificed under ether anesthesia. Blood samples were collected prior to sacrifice to determine the fasting blood sugar (FBS) levels and the serum levels of liver function biomarkers, including amino transaminases (ALT, AST),

alkaline phosphatase (ALP), and albumin (Alb), using commercially available kits (Pars Azmon, Iran) and an automatic biochemistry analyzer (bench-top-BT 3000 PLUS, Italy).

**3.5.2. Antioxidant assays, estimation of lipid peroxidation levels, and histopathological examinations.** Autopsies of livers were immediately performed after sacrificing the rats, followed by rinsing with ice-cold isotonic saline and blotting dry. The liver tissue was then comminuted and homogenated.<sup>57</sup> Assessments of hepatic tissue superoxide dismutase (SOD) and glutathione peroxidase (GPx) activities were carried out according to kit instructions (Randox Labs., UK), which have been described previously.<sup>58</sup> The lipid peroxidation levels in the homogenized liver tissue samples were estimated based on the formation of thiobarbituric acid reactive substances (TBARS); this has been described previously.<sup>59,60</sup> Following sacrifice, the liver was removed and washed in ice-cold saline to remove the blood. Then, it was immediately transferred to a 10% formalin fixative, dehydrated using a graded alcohol series, imbedded in paraffin, cut into 5  $\mu\text{m}$  thick segments, and finally stained with hematoxylin and eosin (H&E). The slides were examined *via* light microscopy to observe microscopic changes of pathological significance.<sup>57</sup>

## 4. Conclusions

In summary, we have described a simple biosynthetic method for the preparation of Ag and NiO nanoparticles using aqueous VPLe. Both types of nanoparticle were successfully characterized with different techniques. Therefore, this herb is shown to be a pollutant-free and potent biogenerator of these nanoparticles under aerobic conditions. According to our results, we may claim that VPLe can improve the condition of rats with diabetic hepatopathy *via* a decrease in oxidative stress and an enhancement in the activities of antioxidant enzymes in the liver.

## Conflicts of interest

There are no conflicts to declare.

## Acknowledgements

This research was financially supported by Sabzevar University of Medical Sciences and Hakim Sabzevari University.

## References

- 1 M. V. Yezhelyev, X. Gao, Y. Xing, A. Al-Hajj, S. Nie and R. M. O'Regan, *Lancet Oncol.*, 2006, 7(8), 657–667.
- 2 F. Mohammadi, M. Yousefi and R. Ghahremanzadeh, *Adv. J. Chem., Sect. A*, 2019, 2(4), 266–275.
- 3 N. Ahmad, S. Sharma, M. K. Alam, V. N. Singh, S. F. Shamsi and B. R. Mehta, *Colloids Surf., B*, 2010, 81, 81–86.
- 4 M. Sathishkumar, K. Sneha, S. W. Won, C. W. Cho, S. Kim and Y. S. Yun, *Colloids Surf., B*, 2009, 73, 332.
- 5 B. Mahdavi, S. Saneei, M. Qorbani, M. Zhaleh, A. Zangeneh, M. M. Zangeneh, E. Pirabbasi, N. Abbasi and H. Ghaneialvar, *Appl. Organomet. Chem.*, 2019, 5164.



- 6 S. S. Shankar, A. Rai, A. Ahmad and M. J. Sastry, *J. Colloid Interface Sci.*, 2004, **275**, 496.
- 7 F. Thema, E. Manikandan and A. Gurib-Fakim, *J. Alloys Compd.*, 2016, **657**, 655–661.
- 8 N. Thovhogi, A. Diallo and A. Gurib-Fakim, *J. Alloys Compd.*, 2015, **647**, 392–396.
- 9 F. Thema, E. Manikandan and M. Dhlamini, *Mater. Lett.*, 2015, **161**, 124–127.
- 10 M. Ovais, A. T. Khalil and A. Raza, *Nanomedicine*, 2016, **12**, 3157–3177.
- 11 P. Laokul, V. Amornkitbamrung, S. Seraphin and S. Maensiri, *Curr. Appl. Phys.*, 2011, **11**, 101.
- 12 S. B. Manjare, S. G. Sharma, V. L. Gurav, M. R. Kunde, S. S. Patil and S. R. Thopate, *Asian J. Nanosci. Mater.*, 2019, DOI: 10.26655/AJNANOMAT.2020.1.6.
- 13 N. H. Idiris, J. Z. Wang, S. Chou, C. Zhong, Md. M. Rahman and H. Liu, *J. Mater. Res.*, 2011, **26**, 860.
- 14 J. R. Richardson, D. I. Yiagas, B. Turk, K. Forster and M. V. Twigg, *J. Appl. Phys.*, 1991, **70**, 6977.
- 15 S. Mohanraj, p. Vanathi, N. Sowbarniga and D. Saravanan, *Indian J. Fibre Text. Res.*, 2012, **37**, 389.
- 16 V. R. Tandon and R. K. Guota, *Indian J. Physiol. Pharmacol.*, 2005, **49**(2), 199–205.
- 17 H. Kirmizibekmez, E. Ariburnu, M. Masullo, M. Festa, A. Capasso, E. Yesilada and S. Piacente, *Fitoterapia*, 2012, **83**(1), 130–136.
- 18 R. P. Samy, S. Ignacimuthu and A. Sen, *J. Ethnopharmacol.*, 1998, **62**, 173–182.
- 19 R. S. Telang, S. Chatterjee and C. Varshneya, *Indian J. Pharmacol.*, 1999, **31**, 363–366.
- 20 R. Manikandan, R. Sundaram, P. Srinivan, S. Beulaja and C. Arulvasu, *Int. J. Pharm. Anal.*, 2009, **2**, 4–10.
- 21 M. Umamaheswari, K. Asokumar, A. Somasundaram, T. Sivashanmugam, V. Subhadradevi and T. K. Ravi, *J. Ethnopharmacol.*, 2007, **109**, 547–551.
- 22 M. I. Alam, *J. Ethnopharmacol.*, 2003, **86**, 75–80.
- 23 W. Woradulayapinij, N. Soonthonharenonn and C. Wiwat, *J. Ethnopharmacol.*, 2005, **101**, 84–89.
- 24 C. Arulvasu, D. Prabhu, R. Manikandan, P. Srinivasan, S. Sellamuthu and D. Dinesh, *Int. J. Drug Discovery*, 2010, **2**(1), 1–7.
- 25 R. Tayebbe, E. Filehkesh and V. Amani, *Asian J. Chem.*, 2007, **19**(3), 1772.
- 26 Th. I. Shaheen, M. E. El-Naggar, J. S. Hussein, M. El-Bana, E. Emara, Z. El-Khayat, M. M. G. Fouda, H. Ebaid and A. Hebeish, *Biomed. Pharmacother.*, 2016, **83**, 865.
- 27 S. M. El-Sayed, M. E. El-Naggar, J. Hussein, D. Medhat and M. El-Banna, *Colloids Surf., B*, 2019, **184**, 110465.
- 28 J. Hussein, M. F. Attia, M. El Bana, S. M. El-Daly, N. Mohamed, Z. El-Khayat and M. E. El-Naggar, *Int. J. Biol. Macromol.*, 2019, **140**, 1305.
- 29 R. A. Hussein, A. A. A. Salama, M. E. El Naggar and G. H. Ali, *Biocatal. Agric. Biotechnol.*, 2019, **20**, 101237.
- 30 J. Hussein, M. E. El-Naggar, Y. AbdelLatif, D. Medhat, M. El Bana, E. Refaat and S. Morsy, *Colloids Surf., B*, 2018, **170**, 76.
- 31 J. Hussein, M. El-Banna, T. Abdel Razik and M. E. El-Naggar, *Int. J. Biol. Macromol.*, 2018, **107**, 748.
- 32 D. Medhat, J. Hussein, M. E. El-Naggar, M. F. Attia, M. Anwar, Y. Abdel Latif, H. F. Booles, S. Morsy, A. Razik Farrag, W. K. B. Khalil and Z. El-Khayat, *Biomed. Pharmacother.*, 2017, **91**, 1006.
- 33 M. C. Blendea, M. J. Thompson and S. Malkani, *Clin. Diabetes*, 2010, **28**(4), 139–144.
- 34 K. Kumar, S. Mehershahi, C. Chime, H. Tariq, S. K. Nayudu and S. Chilimuri, *Case. Rep. Gastroenterol.*, 2018, **12**(2), 466–472.
- 35 F. Stickel and D. Schuppan, *Dig. Liver Dis.*, 2007, **39**(4), 293–304.
- 36 H. Yaribeygi, M. T. Mohammadi and A. Sahebkar, *Biomed. Pharmacother.*, 2018, **98**, 333–337.
- 37 S. Bansal, D. Chawla, M. Siddarth, B. D. Banerjee, S. V. Madhu and A. K Tripathi, *Clin. Biochem.*, 2013, **46**(1–2), 109–114.
- 38 J. Mohamed, A. H. Nazratun Nafizah, A. H. Zariyantey and S. B. Budin, *Sultan Qaboos Univ. Med. J.*, 2016, **16**(2), 132–141.
- 39 E. Mansouri, M. Panahi, M. A. Ghaffari and A. Ghorbani, *Iran. Biomed. J.*, 2011, **15**(3), 100–106.
- 40 E. W. C. Chan, S. K. Wong and H. T. Chan, *J. Integr. Med.*, 2018, **16**(3), 147–152.
- 41 T. Movahhed Haghighi, M. J. Saharkhiz, A. R. Khosravi, F. Raouf Fard and M. Moein, *Ind. Crops Prod.*, 2017, **109**, 53–59.
- 42 M. Mozdianfard, M. Akhbari and H. Batooli, *Nat. Prod. Res.*, 2012, **26**(23), 2162–2167.
- 43 H. Akhlaghi, *J. Chem. Health Risks*, 2017, **7**, 3.
- 44 H. ahmadvand, H. amiri, S. Ekbatan Hamadani and S. Bagheri, *Sci. Mag. Yafte.*, 2012, **14**(2), 5–13.
- 45 V. Nayagam, K. Palanisamy and D. Thiraviadoss, *Asian J. Nanosci. Mater.*, 2019, **2**(3), 301–313.
- 46 M. A. Nasser, M. Shahabi, A. Allahresani and M. Kazemnejadi, *Asian J. Green Chem.*, 2019, **3**(3), 382–390.
- 47 M. B. Ahmad, M. Y. Tay, K. Shameli, M. Z. Hussein and J. J. Lim, *Int. J. Mol. Sci.*, 2011, **12**, 4872.
- 48 M. B. Ahmad, K. Shameli, M. Darroudi, W. M. Z. Wan Yunus and N. A. Ibrahim, *Am. J. Appl. Sci.*, 2009, **6**, 1909.
- 49 G. E. Snopatin, M. Yu, M. Matveeva and G. G. Butsyn, *Inorg. Mater.*, 2006, **42**, 1388–1392.
- 50 A. Zarei, G. Vaezi, A. A. Malekirad and M. Abdollahi, *Avicenna J. Phytomed.*, 2015, **5**(2), 138–147.
- 51 F. Hussain, A. Malik, U. Ayyaz, H. Shafique, Z. Rana and Z. Hussain, *Asian Pac. J. Trop. Med.*, 2017, **10**(11), 1054–1058.
- 52 N. A. Mat-Rahim, T. H. Lim, N. A. Nor-Amdan and S. AbuBakar, *J. Evidence-Based Complementary Altern. Med.*, 2017, 6125829.
- 53 S. M. Kalbolandi, A. V. Gorji, H. Babaahmadi-Rezaei and E. Mansouri, *Mol. Biol. Rep.*, 2019, **46**(4), 4039–4047.
- 54 E. A. Oshaghi, I. Khodadadi, F. Mirzaei, M. Khazaei, H. Tavilani and M. T. Goodarzi, *J. Pharm.*, 2017, 6081374.



- 55 R. Kumar, *Indian J. Endocrinol. Metab.*, 2018, **22**(4), 552–559.
- 56 Y. Avadhoot and A. C. Rana, *Arch. Pharmacol. Res.*, 1991, **14**(1), 96–98.
- 57 E. Mansouri, L. Khorsandi and H. A. Abedi, *Iran. J. Basic Med. Sci.*, 2014, **17**(6), 460–464.
- 58 M. M. Bradford, *Anal. Biochem.*, 1976, **72**, 248–254.
- 59 E. Mansouri, M. Panahi, M. A. Ghaffari and A. Ghorbani, *Iran. Biomed. J.*, 2011, **15**, 100–106.
- 60 E. A. Golod and A. B. Gershman, *Urologiia i nefrologiia*, 1989, **4**, 50–55.

